A model predicting sheet charge density and threshold voltage with dependence on interface states density in LM−InAlN/GaN MOSHEMT

© Devashish Pandey¶, T.R. Lenka¶¶

Department of Electronics and communication Engineering, National Institute of Technology Silchar, 788010 Assam, India

(Получена 11 марта 2014 г. Принята к печати 10 апреля 2014 г.)

Trap densities in oxide/semiconductor interface are very crucial factor in deciding the performance of HEMT devices. Its effect cannot be overlooked which though have negligible effect below a particular value can degrade the performance of the device at higher values. In this regard a model is presented relating important parameters like surface potential, sheet charge concentration and threshold voltage in relation to the number of density of states in lattice matched (LM) $In_{0.17}Al_{0.83}N$/GaN based MOSHEMT. The model explains phenomena like current collapse and surface potential pinning which further leads to threshold voltage pinning that can lead to serious problems in HEMTs. An insight on the preference of metal to be used as a gate metal is also provided.

1. Introduction

IN RECENT years GaN based HEMTs have attracted a lot of attention. Incorporation of a barrier layer (AlN, AlGaN, InGaN, InAlN etc.) over the channel layer (GaN) has resulted in a high 2DEG density greaterthan 10^{13} cm^{-2} resulting in a high current density responsible for a high power output. $In_{0.17}Al_{0.83}N$ is the recent contender as a barrier layer providing a high current density greater then 1 A/mm with high frequency and high temperatureoperation [1–4]. A 17% Indium content in the barrier assures a perfect lattice matching with the GaN making it possible to incorporate very thin barriers (10 nm) without affecting the 2DEG charge density. These thin barriers results in high leakage current that can be reduced by introducing thin oxide which results in a MOSHEMT structure.Introduction of the oxide results in the formation of interface trap densities the probability of which are given by (1) and (2) for donor and acceptor trap densities respectively. Where E_d and E_a is the energy of the donor and acceptor state respectively with respect to the valence band edge,

$$F_{SD}(E_d) = \frac{1}{1 + 2\exp\left(\frac{E_F - E_d}{kT}\right)}, \quad (1)$$

$$F_{SA}(E_a) = \frac{1}{1 + 4\exp\left(\frac{E_a - E_F}{kT}\right)} \quad (2)$$

E_F — Fermi level, k — Boltzmann's constant and T is temperature.

The energy level of the interface states are fixed relative to the semiconductor band edge at the interface, so when the surface potential changes, the occupation probability of the interface states will also change, according to the relative position of the Fermi-level and the energy level of the interface states. Thus it becomes a very sensitive parameter to the surface potential which is directly related to the applied gate to source voltage. These interface states also effect the pinch off voltage of the device and make it a variable to the charged interface states.Due to a strong dependence of the interface state density on some important parameters of the device like threshold voltage and sheet charge concentration a need for an efficient model arises. There are only a few limited physics-based analytical models available for AlGaN/GaN MODFETs that attempts to model the 2DEG density [5,6]. Not much of the work in this subject is being done on the $In_{0.17}AlN_{0.83}$/GaN MOSHEMTs as yet. In this paper an attempt is made to model these important parameters with their dependence on the interface state density and to show how crucial its effect can be on the device performance. Analysis starts with section 2 with the description of the proposed device structure along with a linking concept to the model development which is discussed in section 3. Section 4 gives more insight into the equations developed in the previous section with the help of plots and their discussions which is followed by conclusion in section 5.

2. MOSHEMT structure

Fig. 1 is the MOSHEMT structure [7] that is to be analyzed. 2.5 nm of barrier layer (InAlN) is deposited by MOCVD over a 200 nm channel layer (GaN). A 1600 nm Fe doped GaN layer serves as a semi-insulating layer while SiC is used as a substrate. 4.5 nm of SiO_2 is deposited over InAlN that acts as an insulating layer. The condition of the conduction band of this heterojunction in absence of oxide under zero bias is given in Fig. 2. $In_{0.17}Al_{0.83}N$/GaN based HEMTs follow nearly the same physics involved in their predecessor $Al_xGa_{(1-x)}N$/GaN except that in the latter the effect of piezoelectric polarization is also taken into consideration other than spontaneous polarization. In $In_{0.17}Al_{0.83}N$/GaN (with 17% Indium content) since the layers are perfectly lattice matched the structure is not under strain as a result there is no piezoelectric polarization. But

¶ E-mail: devashishpandev21@gmail.com
¶¶ E-mail: trlenka@gmail.com

since the mole fraction of Aluminum here can be increased without sacrificing the lattice matching we get a very high degree of spontaneous polarization.

The 2DEG concentration for a MESHEMT configuration is given by [8]

$$n_s = \sigma_{pol} - \frac{\varepsilon_{\mathrm{AlInN}}}{q d_{\mathrm{AlInN}}} [\phi_S + E_F(N_S) - \Delta E_C]. \qquad (3)$$

Where σ_{pol} is the maximum limit of concentration due to spontaneous polarization which is taken to be $3.3 \cdot 10^{13}\,\mathrm{cm}^{-2}$. The trapezoidal shape of the conduction band of $In_{0.17}Al_{0.83}N$ is attributed to the fact that the polarization fields extends from the $In_{0.17}Al_{0.83}N$/GaN interface towards the metal/$In_{0.17}Al_{0.83}N$ interface resulting in a 2DEG formation at the $In_{0.17}Al_{0.83}N$/GaN interface to preserve the charge neutrality. ϕ_S is the surface potential, $E_F(N_S)$ is the energy difference between Fermi level and the electron with minimum energy involved in the formation of 2DEG, ΔE_C is the offset in the conduction band and dInAlN is the barrier thickness.

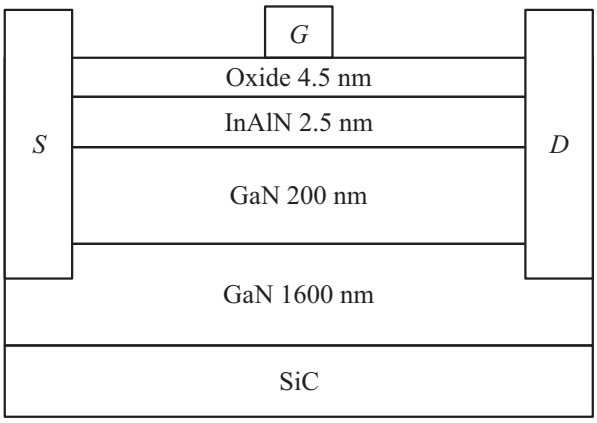

Figure 1. The $In_{0.17}Al_{0.83}N$/GaN MOSHEMT structure.

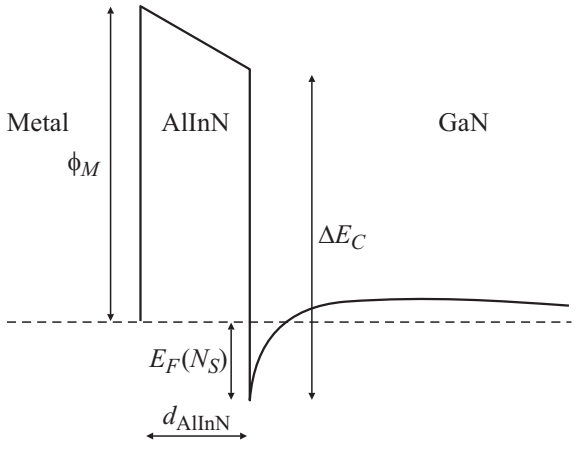

Figure 2. Conduction band of $In_{0.17}Al_{0.83}N$/GaN heterojunction under zero bias.

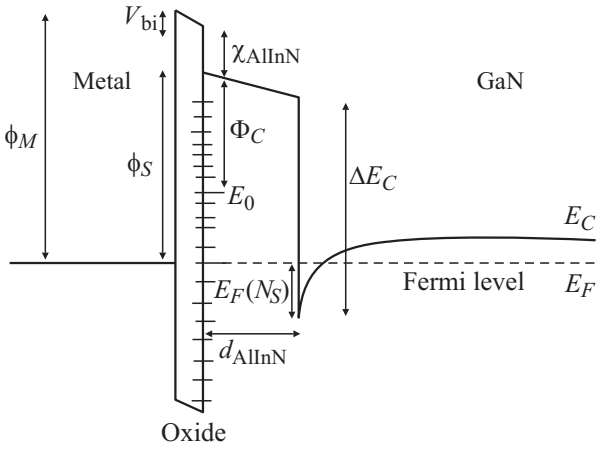

Figure 3. Conduction band for Metal−Oxide−$In_{0.17}Al_{0.83}N$−GaN heterostructure.

3. Model development

Fig. 3 depicts the conduction band of the proposed HEMTstructure in Fig. 1 for metal−oxide−$In_{0.17}Al_{0.83}N$−GaN heterojunction. With the introduction of the gate dielectric we can expect some non-idealities at the oxide/$In_{0.17}Al_{0.83}N$ interface arising due to incomplete oxidation or non-ideal fabrication process which results in the incorporation of the negatively charged oxygen species along with some positive charged ions formed due to the unsatisfied bonds. Also there are uncompensated donor charges by mobile ionic charges and fixed charges trapped within the oxide and itself, which are often created during the fabrication process. The donor charges can also be attributed to the fact that the negative charge density has to be compensated by an equal positive charge to maintain the charge neutrality in the structure. The above are the causes that lead to the formation of a large density of donor and acceptor states in the oxide/$In_{0.17}Al_{0.83}N$ interface. Thedensities of states affect the threshold voltage and the total sheet charge density which govern the basic modeling equations of HEMT.

A. Determining surface potential (ϕ_S)

Let us assume that the interface states density at the oxide/$In_{0.17}Al_{0.83}N$ interface be $D_{\mathrm{st}} = 10\,\mathrm{eV}^{-1} \cdot \mathrm{m}^{-2}$. E_0 here is the neutral level, which implies, that all the interface levels below it are donor traps while above it are acceptor traps. Since all the levels above Fermi level are unoccupied all the donor levels between the neutral level E_0 and the Fermi level E_F are ionized contributing a charge

$$Q_{\mathrm{st}} = D_{\mathrm{st}} q (E_0 - E_F). \qquad (4)$$

Due to this charge a constant electric field is set up in the oxide towards the metal which leads to a voltage drop of Vbi. Since there are charges present in the interface of the

oxide it can be seen as a capacitance with oxide as the dielectric therefore

$$V_{\text{bi}} = \frac{Q_D + Q_{\text{st}}}{C_{\text{oxide}}}. \quad (5)$$

Where Q_D is the depletion charge and Q_{st} is the charge due to the ionized donors. C_{oxide} is the oxide capacitance. The depletion charge is given by

$$Q_D = qN_D d_{\text{AlInN}}, \quad (6)$$

where N_D is the donor impurity concentration in $In_{0.17}Al_{0.83}N$. Substituting the value of Q_D and Q_{st} from Eqs (3) and (5) into Eq. (4) we get

$$V_{\text{bi}} = \frac{qN_D d_{\text{AlInN}} + D_{\text{st}} q(E_0 - E_F)}{C_{\text{oxide}}}. \quad (7)$$

Now from Fig. 3

$$\phi_S = \phi_M - \chi_{\text{AlInN}} - V_i \quad (8)$$

and

$$E_0 - E_F = \phi_S - \phi_0. \quad (9)$$

Substituting the value of V_{bi} from Eq. (6) into Eq. (7) and making use of (8) we get

$$\phi_S = \frac{\phi_M - \chi_{\text{AlInN}} - \frac{qN_D d_{\text{AlInN}}}{C_{\text{oxide}}}}{1 + \frac{D_{\text{st}} q}{C_{\text{oxide}}}}. \quad (10)$$

Which can be reduced to the following form

$$\phi_S = \gamma(\phi_M - \chi_{\text{AlInN}}) + (1 - \gamma)\phi_0 - \frac{\gamma q N_D d_{\text{AlInN}}}{C_{\text{oxide}}}, \quad (11)$$

where

$$\gamma = \frac{1}{1 + \frac{D_{\text{st}} q}{C_{\text{oxide}}}}. \quad (12)$$

B. Determining sheet charge concentration (n_s)

Substituting the value of ϕ_S from Eq. (11) in Eq. (3) we get a very detailed dependence of the sheet charge concentration on various parameters

$$n_s = \sigma_{pol} - \frac{\varepsilon_{\text{AlInN}}}{q d_{\text{AlInN}}}\left[\gamma(\phi_M - \chi) + (1 - \gamma)\phi_0 - \frac{\gamma q N_D d_{\text{AlInN}}}{C_{\text{oxide}}} + E_F(N_S) - \Delta E_C\right]. \quad (13)$$

The self-consistent solution of the Schrodinger's and Poisson's equations in the assumption that only two of the subbands in the triangular well (E_0 and E_1) are occupied

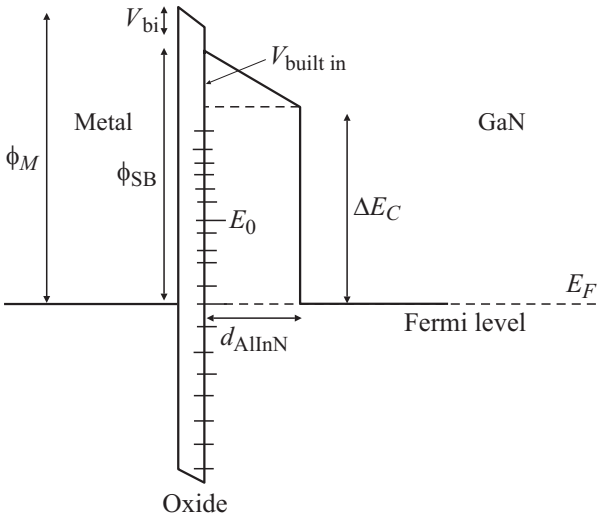

Figure 4. Conduction band at pinch off depicting the condition $E_F(N_S) = 0$.

gives the sheet charge concentration in the potential well as [9]

$$n_s = DkT \sum_{i=0,1} \ln\left(1 + \exp\left(\frac{E_F(N_S) - E_i}{kT/q}\right)\right). \quad (14)$$

Where $D = 4\pi m^*/h^2$ is the conduction band density of states of a 2D system, m^* is the electron effective mass, h is the Planck's constant, k is the Boltzmann's constant, T is the ambient temperature, $E_0 = c_0 n_s^{2/3}$ (in electronvolts), and $E_1 = c_1 n_s^{2/3}$ (in electronvolts) are the allowed energy levels in the well. Here c_0 and c_1 are determined by Robin boundary condition [10,11]. A second-order expression which gives a good fit to the numerical solution of (14) when E_F has been given by Kola et al. [9] where k_1, k_2 and k_3 has been calculated by [10]

$$E_F(N_S) = k_1 + k_2 n_s^{1/2} + k_3 n_s. \quad (15)$$

Making use of (15) in (1) and solving for ns we get

$$n_s = \left[-\frac{Y}{X} + \sqrt{\left(\frac{Y}{X}\right)^2 - \frac{2Z}{X}}\right]^2, \quad (16)$$

where X, Y and Z have the following expressions

$$X = 2(\varepsilon_{\text{AlInN}} k_3 + q d_{\text{AlInN}}), \quad (17)$$

$$Y = \varepsilon_{\text{AlInN}} k_2, \quad (18)$$

$$Z = \varepsilon_{\text{AlInN}}(k_1 + \phi_s - \Delta E_C) - q d_{\text{AlInN}} \sigma_{pol}. \quad (19)$$

Where the value of ϕ_S is used from (11) to complete the equation.

C. Determining threshold voltage (V_T)

When a voltage is applied at gate a point comes when the channel gets totally devoid of electrons as a result the sheet charge density becomes zero. The channel is then said to be pinched off Fig. 4 shows a pinched off channel. Substituting $n_S = 0$; $E_F(N_S) = 0$ and $\phi_S = \phi_{SB} - V_g$ in (16) we get

$$V_T = \gamma(\phi_M - \gamma_{AlInN}) + (1-\gamma)\phi_0 - \frac{\gamma q N_D d_{AlInN}}{C_{oxide}} - \Delta E - \frac{\sigma_{pol} q d_{AlInN}}{\varepsilon_{AlInN}}. \quad (20)$$

Where γ is given by (12). This relation also shows a dependence of the threshold voltage on Dst. Thus it can be seen that important parameters are affected with the variation of the D_{st} and thus it is a crucial factor in deciding the performance of HEMT devices.

4. Results and discussions

The equations deduced above are now plotted to see the outcome of the dependence of the various parameters like the suface potential, sheet charge concentration and threshold voltage with D_{st}. In all the analysis value of ϕ_0 is assumed to be 1.2 eV while all the other parameters are given the default values as found in most of the literature. The oxide that we used here is SiO_2 so the values of dielectric constant will apply to it. Fig. 5 represents the plot of (11) as a graphical representation of the variation of surface potential with respect of the density of states. The graph has been plotted for different metals to outline the usefulness of the gate metal that can be used. We see here how the surface potential is constant up to a particular value of D_{st}, which is ideally the case but as the density of states increases we see a steep roll off in the surface potential. Ideally it is believed that surface potential and the metal work function are linearly related. This notion is true, but only till a particular limit of the number of density of states beyond which the linearity breaks down.

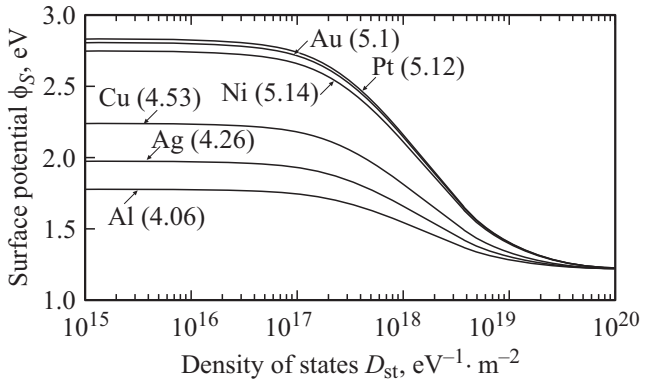

Figure 5. A plot of surface potential vs density of states for different metals. Their respective work functions are given in the bracket.

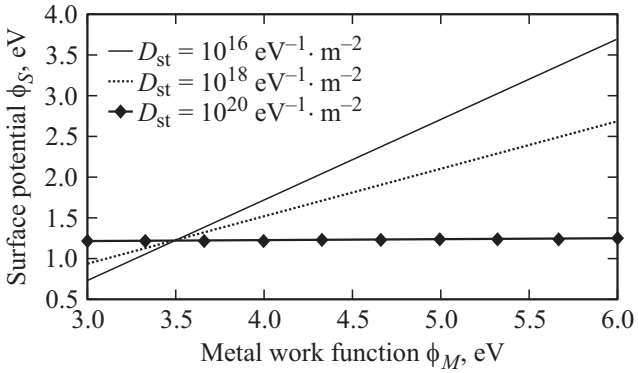

Figure 6. Graph depicting relation between surface potential and metal work function for different values of density of states.

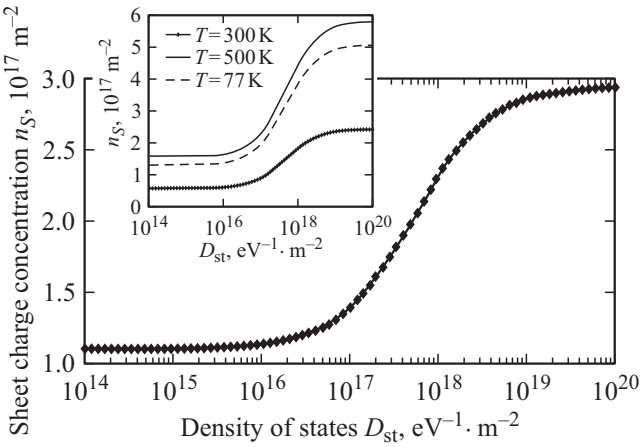

Figure 7. Sheet charge concentration relating density of states at $T = 300$ K. Inset shows the same relation at $T = 77$, 300 and 500 K.

This is shown in Fig. 6, where surface potential and metal work function are plotted at constant values of D_{st} and exhibit linear behavior at $D_{st} = 10^{16}\,\text{eV}^{-1}\cdot\text{m}^{-2}$ and $D_{st} = 10^{18}\,\text{eV}^{-1}\cdot\text{m}^{-2}$. But at $D_{st} = 10^{20}\,\text{eV}^{-1}\cdot\text{m}^{-2}$ surface potential is pinned to a constant value irrespective of the value of metal work function. This is a serious problem in HEMT devices.

Sheet charge density is also a sensitive parameter to the number of D_{st}. In this paper the analysis is donor trap based and so the results are plotted accordingly. For acceptor trap densities same analysis will follow but with different outcome altogether. This analysis led us to (16), the result of which is plotted in Fig. 7. It depicts the sensitivity of sheet charge concentration with respect to the density of states. The curve starts with a constant value and after approximately $D_{st} = 10^{16}\,\text{eV/m}^2$ the concentration is effected by the number of density of states making it dependent on D_{st}. So even ns cannot be treated as a constant. The effect of trap density on the sheet charge concentration is even more profound under a constant change in the polarity of gate voltage. This

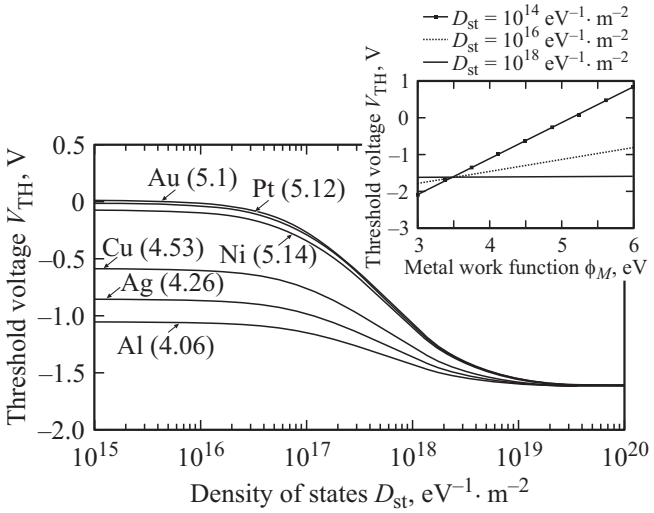

Figure 8. Threshold voltage variation with the number of density of states. Plot of threshold voltage with respect to metal work function for constant value of $D_{st} = 10^{16}$, 10^{18}, 10^{20} eV$^{-1}\cdot$ m^{-2} is shown in the inset.

change gives rise to an undesirable phenomena known as current collapse [12,13] deteriorating the transient behavior of HEMT devices. A rough estimate of the temperature dependence can also be deduced from (16) by using values of temperature dependent parameters k_1, k_2 and k_3 at three specific temperatures 77, 300 and 500 K [10]. The inset of Fig. 7 gives the plotted result. Switching the device on and off after and before a particular value without encountering any non idealities is a very challenging task before a device engineer. This value termed as threshold voltage was deduced in (20) as a function of number of density of states.

Plotting it gives us an idea as to how the variation of threshold voltage takes place with the variation of number of density of states. The result is plotted in Fig. 8 and it can be seen that the threshold voltage is unchanged till a particular value of number of density of states($\sim 10^{16}$ eV$^{-1}\cdot$ m^{-2}) after which it starts to roll off steeply. This can be seen to be applicable equally for all the metals used for the analysis. All the above result pronounce one thing clearly, that, till a particular value of density of states the parameters are generally independent of the number of density of states. So the acceptable value of Dst is approximately below 10^{16} eV$^{-1}\cdot$ m^{-2} after which the device performance is predicted to be effected.

A plot of threshold voltage with respect to the metals with their workfunction ranging from 3 eV to 6 eV and constant D_{st} is made (given in the inset of Fig. 8) to get a clear view from the metal's frame of reference and also to see how the density of states is responsible to pin the threshold voltage to a particular fixed value inspite of the use of different metals with their different work functions (at $D_{st} = 10^{16}$ eV$^{-1}\cdot$ m^{-2}).

5. Conclusion

The model developed can be very useful for getting a deeper insight into the characteristics of MOSHEMTs and can explain several experimentally inexplicable phenomena mathematically. Several approximations are used to avoid lengthy derivations like the height of the channel is not taken into account. Presently the analysis was done independently for donor trap densities so a complete analysis has to be done in relation to even the acceptor trap densities and deducing the result due to the combined effect of the two. Several questions arise after this work as to how does the variation of dielectric effects the performance of the device in relation to D_{st} or how can the variation of height of the channel be incorporated in this model to make it more self-contained. Finding out the solutions to these questions would be our motivation for further research.

References

[1] J. Kuzmik. IEEE Electron Dev. Lett., **22**, 510 (2001).
[2] M. Neuburger, et al. High Speed Electron. Syst., **14** (3), 78 (2004).
[3] F. Medjdoub, et al. Electron. Lett., **42**, 779 (2006).
[4] M. Higashiwaki, et al. Jpn. J. Appl. Phys., **45**, L843 (2006).
[5] Rashmi, A. Kranti, S. Haldar, R.S. Gupta. Sol. St. Electron., **46** (5), 621 (2002).
[6] Rashmi, S. Haldar, R.S. Gupta. Microw. Opt. Technol. Lett., **29** (2), 117 (2001).
[7] Yuanzheng Yue, Zongyang Hu, Jia Guo. Berardi Sensale-Rodriguez, Guowang Li, Ronghua Wang, Faiza Faria, Tian Fang, Bo Song, Xiang Gao, Shiping Guo, T. Kosel, G. Snider, P. Fay, Debdeep Jena, Huili Xing. IEEE Electron. Dev. Lett., **33** (7) (2012).
[8] A.D. Bykhovski, B.L. Gelmont, M.S. Shur. J. Appl. Phys., **81**, 6322 (1997).
[9] S. Kola, J.M. Golio, G.N. Maracas. IEEE Electron. Dev. Lett., **9** (3), 136 (1988).
[10] M. Li, Y. Wang. IEEE Trans. Electron Dev., **55** (1), 261 (2008).
[11] Xiaoxu Cheng, Miao Li, Yan Wang. IEEE Trans. Electron. Dev., **56** (12) (2009).
[12] Ramakrishna Vetury, Naiqain Q. Zhang, Stacia Keller, Umesh K. Mishra. IEEE Trans. Electron. Dev., **48** (3) (2001).
[13] Rongming Chu, Likun Shen, Nicholas Fichtenbaum, Zhen Chen, Stacia Keller, Steven P. DenBaars, Umesh K. Mishra. IEEE Electron. Dev. Lett., **29** (4) (2008).

Редактор Т.А. Полянская